

# Development of a Miniature Multi-Degree-of-Freedom Measurement System for Ultra Precision Stages

Hung-Yu Wang<sup>a</sup>, Bo-Hsun Liao<sup>a</sup>, Ming-Jun Chou<sup>a</sup>, Yang-Yu Tseng<sup>a</sup>, and Kuang-Chao Fan<sup>a</sup>

<sup>a</sup> Department of Mechanical Engineering, National Taiwan University, Taiwan, China

## ABSTRACT

Any linear stage has inherent geometrical errors due to manufacturing errors. The induced Abbé errors have to be compensated for the accuracy of positioning. In addition, although the commercial laser interferometer is capable for the displacement sensing to nanometer resolution, it is, however, bulky in size, expensive in cost and not able to correct the Abbé errors caused by angular errors of the moving stage. In order to minimize and simplify the interferometer as a practically useful sensor for nanopositioning stages in industrial use, this paper presents a newly developed miniature multi-degree-of-freedom measurement system (MDFMS), which is constructed by a wavelength corrected Michelson interferometer and a dual-axis autocollimator. The wavelength correction of the miniature laser interferometer is calibrated by SIOS and controlling the temperature within  $\pm 2$  °C, the wavelength stability is less than  $10^{-6}$ . After calibration, the accuracy of the miniature laser interferometer can reach 32 nm for the travel of 20 mm long. The collimator has accuracy of  $\pm 0.3$  arc-sec within the range of  $\pm 30$  arc-sec. This MDFMS has been integrated into the developed Micro-CMM as a feedback sensor in each axis of the coplanar stage.

**Keywords:** Multi-degree-of-freedom measurement system (MDFMS), Abbé error, Michelson interferometer, wavelength correction, Micro-CMM

## 1. INTRODUCTION

Precision stages are widely used in machine tools, photolithography steppers, precision measuring instrument [1-5]. However, it is extremely difficult to achieve good positioning performance due to assembly errors, component misalignment, control error, and so on. In practice, the performance of high-precision measurement and fabrication machines is constrained by the Abbé principle. The Abbé principle is generally regarded as the most important guideline in the design of precision measuring and production machines. In Bryan's generalized interpretation [6], if the Abbé principle is not possible in the system design, either the slideway that transfers the displacement must be free of angular motion or the angular motion data must be obtained to compensate the Abbé error by software. Following the Abbé principle, Bryan's principle extended the concept to straightness measurement [7].

Laser interferometers are commonly used to detect the displacement of the stage, since they provide a means for attaining high metric resolution and precision, even over long measurement ranges. The versatility and broad applicability of laser interferometers are unattainable using any other metrological methods. Heterodyne laser interferometers are the basis of metrology and control in high accuracy displacement measurement applications. However, it is often very difficult to integrate with machine for on-line measurement because of their large size. Homodyne laser interferometers have some advantage like its ease of use, simple structures and its lower cost. Actually, once the classical errors (stability of the laser source, alignment error, vibration, temperature variation and air turbulence) can be kept small enough, then the practical limitations of interferometry will be given by the noise and the nonlinearity due to optical cross talk [8].

In this report, the miniature multi-degree-of-freedom measurement system is presented. In order to real-time compensate the Abbé error and achieve the nanometer-scale, a miniature multi-degree-of-freedom sensor has been developed not only for measuring the displacement to nanometer resolution but also for detecting the pitch and yaw errors of each axis for Abbé error compensation.

## 2. MULTI-DEGREE-OF-FREEDOM MEASUREMENT SYSTEM

The configuration of the new proposed optical system, named by multi-degree-of-freedom measurement system (MDFMS), is illustrated in Figure 1. In the part of polarizing Michelson interferometer, a partially polarized laser beam of 635 nm wavelength from the laser diode LD impinges on the polarizing beam splitter PBS1 and is split into two beams: the transmitted P-beam and the reflected S-beam. The reflected beam is reflected by the reference mirror, and the transmitted beam is reflected by the moving mirror mounted on the stage. The displacement of the moving mirror will cause the optical path difference between the two reflected beams so as to produce interference.

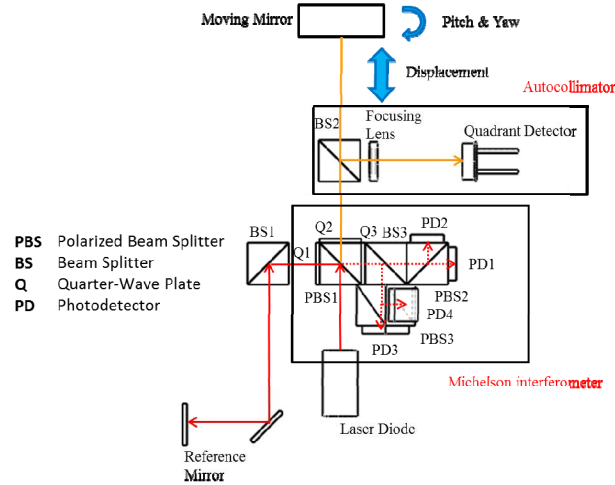


Figure 1. The configuration of the Multi-Degrees-of-freedom measurement system

### 2.1 Michelson interferometer

The optical structure of the Michelson interferometer [9] is shown in the Figure 2. The approximately linearly polarized beam from the laser diode is separated by the polarizing cube beam splitter PBS1. The P-polarized beam passes through and the S-polarized beam is reflected to the left. With careful rotation of the laser diode these two beams will have equal intensity. Then, the quarter waveplates Q1 and Q2 prevent the reflected beams from going back into the laser diode, because each polarization state will be changed by 90° after passing a quarter waveplate twice. The two reflected beams are combined at PBS1 and converted into left and right circularly polarized beams by Q3. With the phase shift module composed by NPBS, PBS2 and PBS3, the interference fringe with 90° phase shift can be detected by photo-detectors PD1 to PD4.

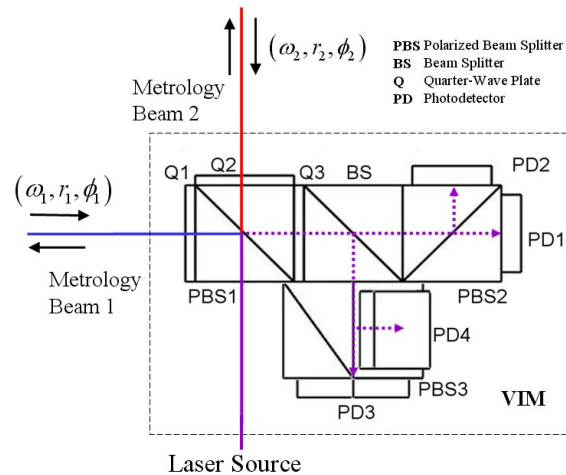


Figure 2. The configuration and optical path of the Michelson interferometer

## 2.2 Autocollimator

According to the principle of optical autocollimator [10] as shown in Figure 3(a) and Figure 3(b), the tilted angle ( $\theta$ ) of the plane mirror will result in the focused spot being shifted laterally by  $2f\theta$ , where  $f$  is the focal length of the focusing lens. The built-in four-quadrant photodiode is used as the beam spot position detector to detect the amount of spot shifts in two axes. The two tilted angles of the plane mirror can then be calculated.

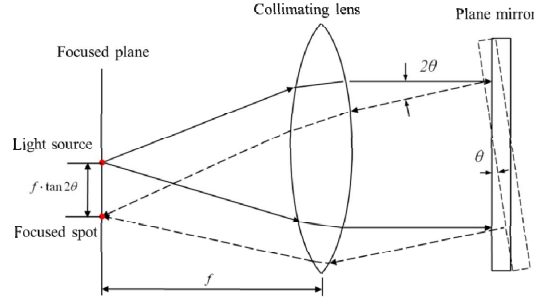


Figure 3(a). The spot movement when the plane mirror is rotated

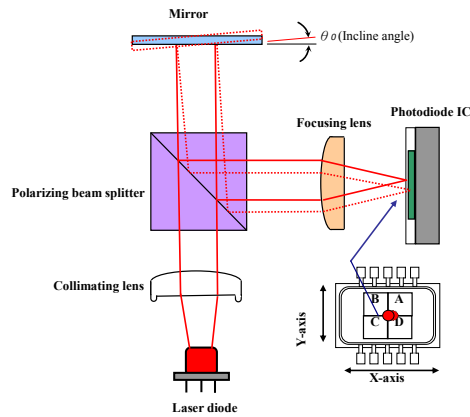


Figure 3(b). The configuration of the autocollimator

Through the current-to-voltage converter with proper resistance, the photocurrent transformed from the photodiode will be converted to voltage for further operation. According to the location of the reflected beam projected onto the four quadrant photodiode, the corresponding voltages to the yaw angle ( $\theta_y$ ) and the pitch angle ( $\theta_x$ ) can be expressed by the following equations, as shown in Figure 4.

$$\theta_x = K_2[(V_A + V_B) - (V_C + V_D)] \quad (1)$$

$$\theta_y = K_2[(V_B + V_C) - (V_A + V_D)] \quad (2)$$

Therefore, the angular errors (pitch and yaw) can be measured by the autocollimator.

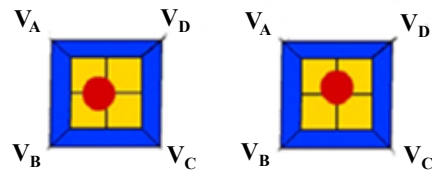


Figure 4. The relationship between the location of the beam spot and voltages (left: yaw, right: pitch)

### 3. SIGNAL PROCESSING

For the positioning measurement up to nanometer resolution, the signal waveform must be corrected to an ideal shape. It may involve substantial computation yet in fast speed. In classical orthogonal waveforms there are three major error sources. As described by Heydemann [12], these are: (1) lack of quadrature ( $\psi$ ), (2) unequal gain in the detector channels ( $a_1 \neq a_2$ ) and (3) DC drift ( $\sigma_1, \sigma_2$ ). Therefore, defective signals of a-b phase occur as the forms of equations below

$$A = a_1 \sin(\theta + \phi) + \sigma_1 \quad (3)$$

$$B = a_2 \cos(\theta) + \sigma_2$$

A signal processing circuit is designed to correct the errors [12]. To correct the first error, vector summation and subtraction is used in order to obtain the exact orthogonal waveforms. The later two errors are corrected by sending the signal through a differential amplifier with appropriate magnification; meanwhile diminishing the common mode noise and DC drift. Figure 5 shows the diagram of signal process circuit.

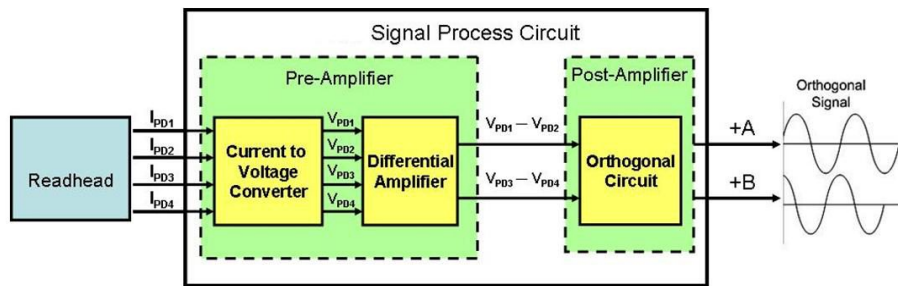


Figure 5. The diagram of signal process circuit

Although the hardware based processor can provide faster process, it cannot deal with complicated computation due to limited memory size. As a result, a real-time signal processing by soft computing is also developed. As shown in Figure 6, the software is able to calculate dynamic waveform errors in real-time. Digital subdivision by arc-tangent function is also included in the software to achieve nanometric resolution. It makes the MDFMS more robust and accurate when the geometrical errors of the moving stage occur.

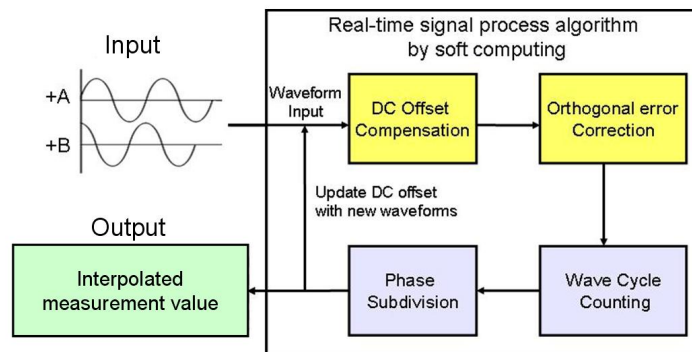


Figure 6. The diagram of real time soft computing

## 4. EXPERIMENT AND RESULTS

### 4.1 Michelson interferometer calibration

#### 4.1.1 Measurement range

The polarizing Michelson interferometer belongs to Homodyne interferometer and constraints on measurement range by the limited coherence length. In order to realize the measurement range, a HP5529A interferometer is employed as a standard. The system and result are shown in the Figure 7(a) and 7(b), respectively. Then, the polarizing Michelson interferometer is workable for the travel range of 35 mm.

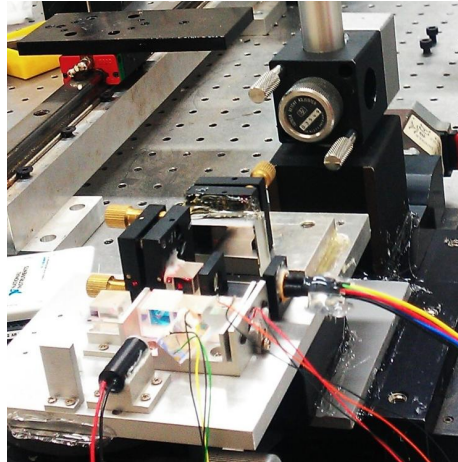


Figure 7(a). The measure range of the Michelson interferometer

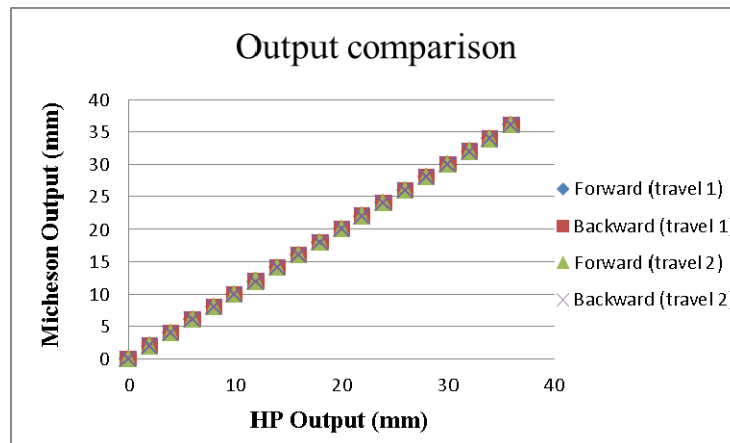


Figure 7(b). The comparison between Michelson interferometer and HP5229A

#### 4.1.2 Accuracy calibration

In order to meet the requirement of nanometer accuracy, this Michelson interferometer is calibrated by a Nanopositioning and Nanomeasuring Machine NMM (SIOS Co.). The calibration system is shown in the Figure 8(a). The Figure 8(b) is the residual error and each target position has been attained five times for the travel range of 25 mm. The positioning error can be controlled to  $\pm 32$  nm with standard deviation 17 nm after cosine error compensation.

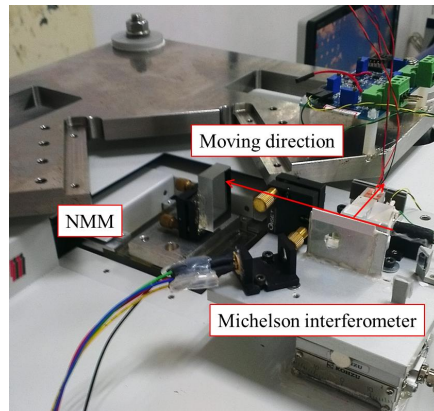


Figure 8(a). The calibration of the Michelson interferometer

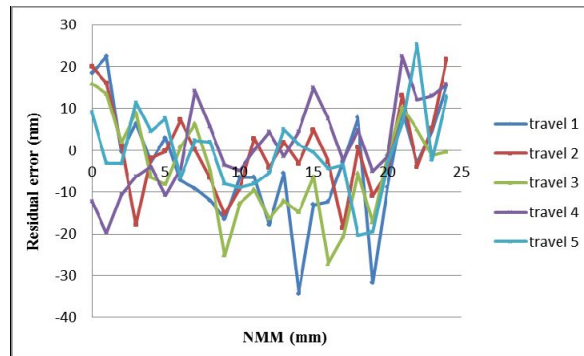


Figure 8(a). Residual errors of the calibration

#### 4.1.3 Wavelength calibration

The accuracy of the Michelson interferometer is affected by wavelength variation. In order to meet the requirement of nanometer accuracy, the wavelength calibration can be introduced by three steps. First, a QPD is employed to adjust the laser beam because the misalignment of the laser beam to the moving axis will cause cosine errors. As shown in Figure 9, the cosine error between the light beam and the moving axis has been adjusted by QPD and the error is 0.052nm. Second, we minimize the Abbé arm to eliminate the influence of Abbé error. Finally, SIOS in the NMM is employed to compare with Michelson interferometer. By fitting the slope of comparison, we could acquire the average wavelength, and eliminate the environment temperature variation. As shown in the Figure 10, the slope is 1.000000 means that the current wavelength has been corrected and the wavelength stability is less than  $10^{-6}$ .

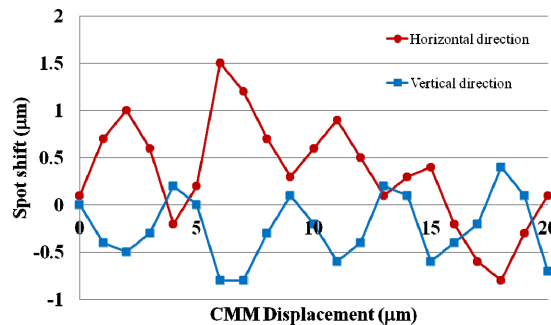


Figure 9. Coaxial adjustment between QPD and CMM stage

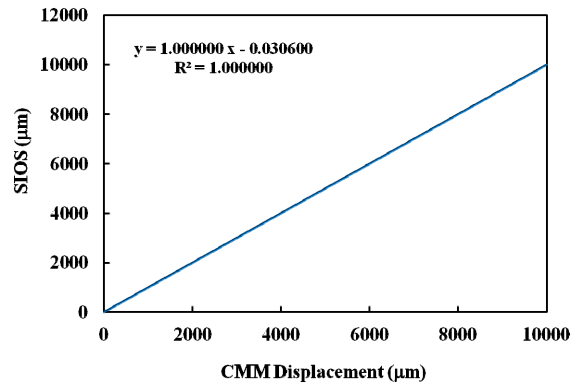


Figure 10. Michelson output compared with SIOS output

#### 4.2 Autocollimator calibration

In order to calibrate the measurement precision, a HP5529A interferometer is employed as a standard. The system is shown in the Figure 11(a). Then with least-square linear fitting the residual errors can be obtained, as shown in Figure 11(b). The residual errors are  $\pm 0.3$  arc-sec within the range of  $\pm 30$  arc-sec.

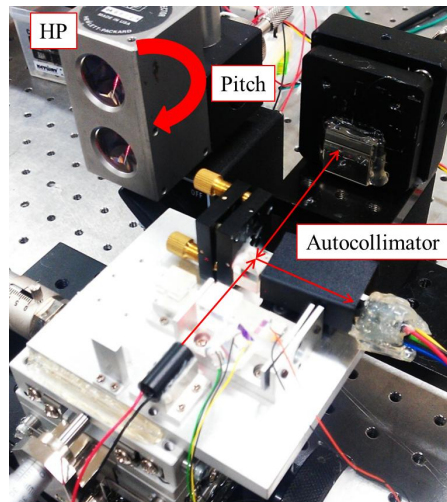


Figure 11(a). The calibration of the Autocollimator

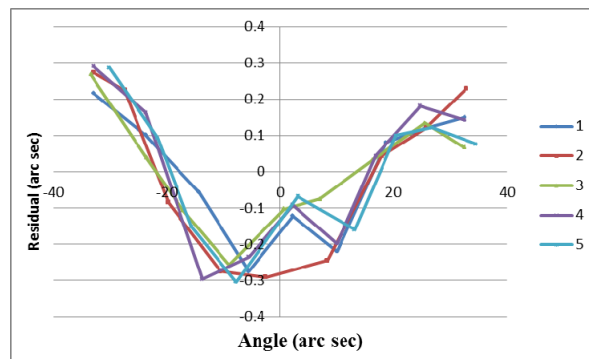


Figure 11(b). Residual errors of the calibration

## 5. CONCLUSIONS

This paper has presented the miniature multi-degree-of-freedom measurement system (MDFMS) comprising a wavelength corrected Michelson interferometer and a dual-axis autocollimator. Using the proposed MDFMS as the feedback sensor, the positioning can achieve 32 nm for the travel of 20 mm long. Besides, the Autocollimator has accuracy of  $\pm 0.3$  arc-sec within the range of  $\pm 30$  arc-sec. The results from experiments verify that the wavelength stability is less than  $10^{-6}$  which under controlling the temperature within  $\pm 2$  °C. Based on these demonstrated experiments, the Micro-CMM has the capability to meet the nanometer accuracy and resolution, as shown in the Figure 12.

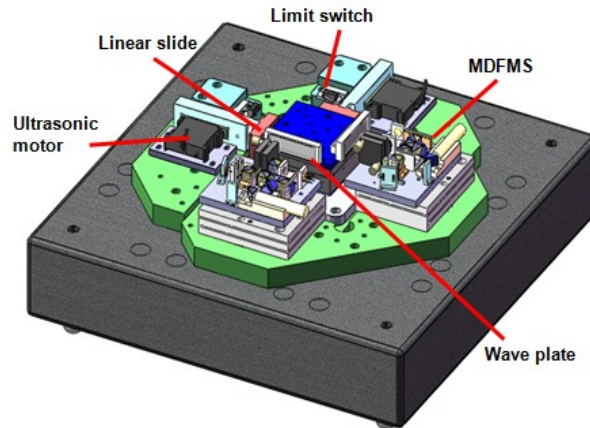


Figure 12. The structure of Micro-CMM

## REFERENCES

- [1] Shamoto, E., Murase, H. and Moriwaki, T., "Ultra-precision 6-axis table driven by means of walking drive," *Annals of CIRP, Papers 49(1)*, 299-302 (2000).
- [2] Fan, K. C., Fei, Y. T., Yu, X. F., Chen, Y. J., Wang, W. L., Cheng, F., and Liu, Y. S., "Development of a low cost Micro-CMM for 3D Micro/nano Measurements," *Measurement Science & Technology, Papers 17(3)*, 524-532 (2006).
- [3] Mckeown, P., "Nanotechnology-special article," *Proc. Nano-metrology in Precision Engineering, Hong Kong*, 5-55 (1998).
- [4] Awaddy, B. A., Shih, W. C. and Auslander, D. M. "Nanometer Positioning of a Linear Motion Stage Under Static Loads," *IEEE/ASME Trans. Mechatron. Papers 3(2)*, 113-119 (1998).
- [5] Fan, K. C., Miao, J. W., Gong, W., Zhang, Y. L. and Cheng, F. "High Precision Measurement System Based on Coplanar XY-stage," *Proc. SPIE 8321(1)*, 1-5 (2011).
- [6] Bryan, J. B. and Carter, D. L. "Design of a new error-corrected co-ordinate measuring machine," *Precision Eng. Papers 1(5)*, 125-128 (1979).
- [7] Zhang, G. X. "A Study of the Abbe principle and Abbe errors," *Annals of CIRP Papers 38(1)*, 525-529 (1989).
- [8] Topcu, S., Chassagne, L., Alayli, Y. and Juncar, P. "Improving the accuracy of homodyne Michelson interferometers using polarization state measurement techniques," *Optics Communications Papers 247*, 133-139 (2005)
- [9] Fan, K. C. and Cheng, F., "High-resolution Angle Measurement based on Michelson Interferometry," *Proc. ICOPEN 19*, 3-8 (2011)
- [10] Wang, H. Y., Fan, K. C., Yen, J. K. and Lin, C. H. "A Long-Stroke Nanopositioning Control System of the Coplanar Stage," *IEEE/ASME Trans. Mechatron. Papers 99*, 1-9 (2013)
- [11] Heydemann, P. L. M., "Determination and correction of quadrature correction of fringe measurement errors in interferometers," *Appl. Opt. Papers 20(19)*, 3382-3384 (1981).
- [12] Fan, K. C. and Lai, Z. F., "An intelligent nano-positioning control system driven by an ultrasonic motor," *Int. J. of Prec. Eng. and Manuf. Papers 9(3)*, 40-45 (2008).